ISSN 0023-1584, Kinetics and Catalysis, 2008, Vol. 49, No. 6, pp. 831–839. © Pleiades Publishing, Ltd., 2008.
Original Russian Text © M.Yu. Smirnov, A.V. Kalinkin, A.A. Dubkov, E.I. Vovk, A.M. Sorokin, A.I. Nizovskii, B. Carberry, V.I. Bukhtiyarov, 2008, published in Kinetika i Kataliz, 2008, Vol. 49, No. 6, pp. 876–885.

Use of the Differential Charging Effect in XPS to Determine the Nature of Surface Compounds Resulting from the Interaction of a Pt/$BaCO_3$/Al_2O_3 Model Catalyst with NO_x

M. Yu. Smirnov[a], **A. V. Kalinkin**[a], **A. A. Dubkov**[b], **E. I. Vovk**[a], **A. M. Sorokin**[a], **A. I. Nizovskii**[a], **B. Carberry**[b], **and V. I. Bukhtiyarov**[a, c]

[a] *Boreskov Institute of Catalysis, Siberian Branch, Russian Academy of Sciences, Novosibirsk, 630090 Russia*
[b] *Ford Forschungszentrum, Aachen, Germany*
[c] *Novosibirsk State University, Novosibirsk, 630090 Russia*
e-mail: smirnov@catalysis.ru

Received February 27, 2008

Abstract—A Pt/$BaCO_3$/Al_2O_3 model NO_x storage–reduction catalyst, which was prepared as a thin film (~100 Å) on the surface of tantalum foil, was studied by X-ray photoelectron spectroscopy (XPS). It was found that the Pt/$BaCO_3$ and Pt/Al_2O_3 catalyst constituents acquired different surface charges in the course of photoelectron emission; that is, differential charging occurred. An analysis of this effect allowed us to determine the nature of the products formed in the interaction of the catalyst with a mixture of NO (260 Pa) + O_2 (2600 Pa) + H_2O (525 Pa) at 250°C followed by reduction with a mixture of CO (2100 Pa) + H_2O (525 Pa) at 450°C. It was found that barium carbonate was converted into barium nitrate as a result of reaction with NO_x on the surface of $BaCO_3$. Simultaneously, platinum supported on both $BaCO_3$ and Al_2O_3 was oxidized. The reduction of the catalyst treated with a mixture containing NO resulted in nitrate decomposition and regeneration of a carbonate coating on the surface of $BaCO_3$; this is accompanied by the reduction of oxidized platinum particles to platinum metal.

DOI: 10.1134/S0023158408060086

INTRODUCTION

The current development of the automobile industry is oriented toward decreasing fuel consumption and reducing carbon dioxide emissions into the atmosphere. In particular, this can be achieved by the use of engines with lean fuel–air mixtures. However, in this case, nitrogen oxides are formed in considerable amounts, and they cannot be efficiently neutralized on the commonly used three-way catalysts with a large excess of oxygen in the reaction mixture. This problem can be solved, in particular, with the use of so-called NO_x storage–reduction (NSR) catalysts developed by Toyota [1]. The principle of operation of the NSR catalyst is the following: initially, in an oxidizing atmosphere, the basic component of the catalyst traps nitrogen oxides as nitrates; then, a short pulse injection of an excess of fuel is performed to increase the amount of reducing gases (CO, H_2, and CH_x) in the exhaust and to reduce the nitrates to nitrogen [1, 2]. Traditionally, BaO, $Ba(OH)_2$, or $BaCO_3$ supported on γ-Al_2O_3 is used as the basic component of the NSR catalyst. Platinum is supported onto the surface of Ba/Al_2O_3 for the more efficient oxidation of NO to NO_2 and then to barium nitrate under oxidizing conditions and for the subsequent nitrate reduction to nitrogen under reducing conditions.

In the past decade, the trapping of NO_x followed by reduction to N_2 on barium-containing NSR catalysts has been intensively studied in order to determine the nature of compounds formed on catalyst surfaces and to elucidate reaction mechanisms; vibrational spectroscopic techniques have been mainly used for this purpose [3–9]. In particular, it was found that the reaction products of NO_x with Pt/BaO/Al_2O_3 are a mixture of nitrites and nitrates coordinated to the catalyst surface in various manners. As a rule, the vibrational spectrum of a product mixture is complex-shaped and bands due to nitrites and nitrates are often difficult to distinguish in this spectrum. Moreover, it cannot be always determined on the surface of which particular catalyst component (Al_2O_3 or BaO) a particular product is localized. Thus, it is of considerable current interest to study these systems by X-ray photoelectron spectroscopy (XPS), which is highly sensitive to the catalyst surface composition and the oxidation states of the constituent chemical elements.

In this work, we used XPS to determine the nature of compounds formed in the interaction of a model NSR catalyst (Pt/$BaCO_3$/Al_2O_3) with nitrogen oxides followed by the reducing regeneration of the catalyst. Additionally, a problem was formulated to examine the applicability of the differential charging effect, which accompanies electron photoemission from dielectric

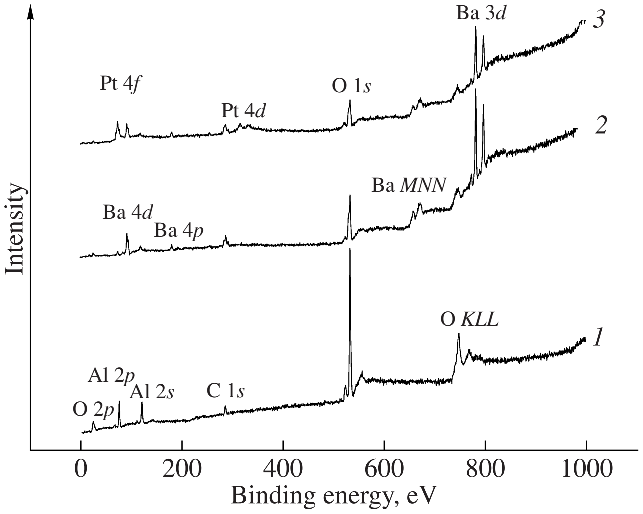

Fig. 1. Survey XPS spectra of (*1*) Al_2O_3, (*2*) $BaCO_3/Al_2O_3$, and (*3*) $Pt/BaCO_3/Al_2O_3$ samples.

samples containing phases with different conductivities [10], to studying surface species formed on the surface of multicomponent systems, in particular, the $Pt/BaCO_3/Al_2O_3$ catalyst.

EXPERIMENTAL

The experiments were performed using a VG ESCA-3 photoelectron spectrometer (United Kingdom) at a residual pressure lower than 5×10^{-7} Pa in the analyzer chamber. Nonmonochromatic MgK_α radiation ($h\nu = 1253.6$ eV) was used to obtain the XPS spectra. The binding energy scale of the spectrometer was precalibrated using the following signal positions of gold and copper metals: Au $4f_{7/2}$ (84.0 eV) and Cu $2p_{3/2}$ (932.6 eV). The treatment of photoemission spectra (the deconvolution into individual components, the measurement of XPS peak areas, and the determination of binding energies) was performed after Shirley background subtraction.

Table 1. Binding energies in the XPS spectrum of the initial $Pt/BaCO_3/Al_2O_3$ sample measured with reference to *BE* of amorphous carbon with consideration for differential charging

Signal	Measured values of *BE*, eV	Corrected values* of *BE*, eV	
		correction for $\Delta_A = 0.3$ eV	correction for $\Delta_B = 3.4$ eV
C 1*s*	285.1	284.8 (+)	281.7 (?)
	288.2	287.9 (?)	284.8 (+)
	292.9	292.6 (?)	289.5 (+)
O 1*s*	531.5	531.2 (+)	528.1 (?)
	534.5	534.2 (?)	531.1 (+)
Al 2*s*	119.9	119.6 (+)	116.5 (?)
Ba $3d_{5/2}$	779.9	779.6 (+)	776.5 (?)
	782.7	782.4 (?)	779.3 (+)
Pt $4f_{7/2}$	72.3	72.0 (+)	68.9 (?)
	75.3	75.0 (?)	71.9 (+)

* Plausible values and values that cannot be assigned to any of the chemical compounds are marked with (+) and (?), respectively.

The sample of Al_2O_3 as a thin film was prepared by evaporation aluminum metal onto a cleaned surface of tantalum foil in an atmosphere of oxygen at 1.3×10^{-3} Pa. Figure 1 shows the survey spectrum of this sample with the specification of the main photoemission signals. In addition to the signals of aluminum and oxygen, it exhibits a C 1*s* signal due to amorphous carbon (or hydrocarbon fragments), which accumulated on the surface during the recording of the spectrum. The absence of signals from the tantalum substrate because of the shielding of the substrate by the alumina film allowed us to estimate the thickness of this film at 100 Å or greater.

Barium carbonate was supported onto an alumina film from a suspension of $BaCO_3$ in ethanol followed by drying in air and calcination in a vacuum at 600°C. Barium carbonate was chosen as the basic component because it is a constituent of commercial NSR catalysts prepared by various procedures [11–13]. Figure 1 (spectrum *2*) also shows the XPS spectrum of a $BaCO_3/Al_2O_3$ sample.

Platinum was supported onto Al_2O_3 or $BaCO_3/Al_2O_3$ by thermal evaporation in a vacuum. Figure 1 (spectrum *3*) shows the survey spectrum of a $Pt/BaCO_3/Al_2O_3$ sample.

The model catalyst samples were treated in the preparation chamber of the spectrometer with a mixture of NO (260 Pa) + O_2 (2600 Pa) + H_2O (525 Pa) (henceforth, this mixture is referred to as NO_x) at 250°C or a regenerating mixture of CO (2100 Pa) + H_2O (525 Pa) at 450°C. Thereafter, they were transferred to the analyzer chamber away from contact with the atmosphere for measuring the spectra. The samples were heated by passing an alternating current through the tantalum foil; the temperature was measured using a Chromel–Alumel thermocouple welded to the reverse side of the foil.

RESULTS AND DISCUSSION

Analysis of the XPS Spectra of the $Pt/BaCO_3/Al_2O_3$ Catalyst in the Initial State

Figure 2 shows the fragments of a spectrum of the initial $Pt/BaCO_3/Al_2O_3$ model catalyst in the regions of C 1*s*, O 1*s*, Ba $3d_{5/2}$, and Pt 4*f* + Al 2*p*. All of the spectra are shown as measured on the instrument, that is, without correcting the scale of binding energies (*BE*) for charging and with no background subtraction, but with deconvolution into individual components. Table 1

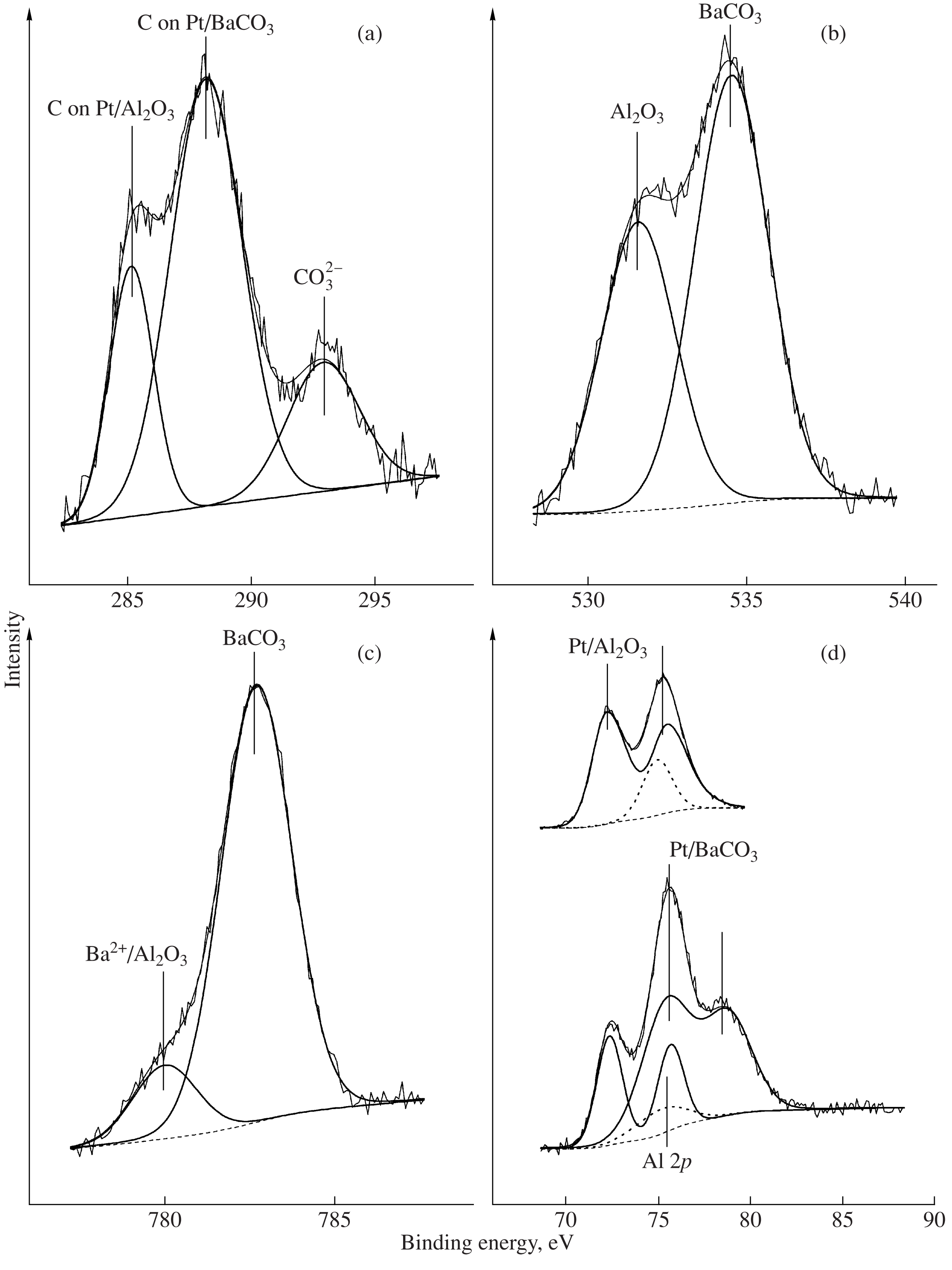

Fig. 2. Fragments of the spectrum of the Pt/BaCO$_3$/Al$_2$O$_3$ model catalyst in the initial state in the (a) C 1*s*, (b) O 1*s*, (c) Ba 3$d_{5/2}$, and (d) Pf 4*f* + Al 2*p* regions without correction for charging and without background subtraction.

summarizes the values of *BE* found based on an analysis of the spectra. Note that the major portion of the elements was represented by two (O 1*s*, Ba 3*d*, and Pt 4*f*) or three (C 1*s*) signals in the spectra; this fact suggests the nonuniform charging of the sample.

In the XPS study of dielectric substances, the surface is charged to a stationary positive potential as a result of electron photoemission; this causes a shift of all signals in the spectrum toward higher binding energies. If a multicomponent system is studied, so-called differential charging can occur when different system components acquire different surface charges as a result of electron photoemission. The charge depends on the resistance of the material (component) and the quality of its electric contact of the phase with the ground. Because of the differential charging, the same element in the same oxidation state as a constituent of different components can exhibit signals with different binding energies in the spectrum.

Usually, the differential charging effect is considered as a negative phenomenon in XPS because it makes difficulties for the correct determination of binding energies [10]. However, in a number of published studies, the differential charging has been successfully used for obtaining valuable information on multicomponent materials [14–20]. A number of approaches have been applied to detect the differential charging and quantitatively evaluate the potential acquired as a result of electron photoemission by individual sample components: the internal standard method [14–16], the controlled surface charging method with the use of an electron gun [17], and the method of varying negative bias in the sample with reference to the ground potential [18].

Let us sequentially analyze individual regions of the XPS spectrum of the initial model catalyst (Fig. 2). Three signals with binding energies of 285.1, 288.2, and 292.9 eV were detected in the C 1*s* region (Fig. 2a). Taking into account the conditions of sample preparation, we can state that one of them should belong to carbon as the constituent of carbonate ions in $BaCO_3$. Moreover, it is well known that amorphous carbon accumulates on the sample surface in the course of measuring the spectrum, and this amorphous carbon is characterized by a C 1*s* signal at a binding energy of 284.5–285.0 eV (in this work, it was 284.8 eV). This signal is commonly used as an internal standard in the calibration of XPS spectra [10]. Because the C 1*s* binding energy of bulk carbonates is 289.5 ± 0.2 eV, it is reasonable to assume that the C 1*s* signal at $BE = 292.9$ eV belongs to carbon as the constituent of the CO_3^{2-} group. Therefore, signals with lower *BE* should be analyzed.

If we assume that the C 1*s* signal at a binding energy of 285.1 eV corresponds to amorphous carbon, the charging value is $\Delta_A = 0.3$ eV. As a result of correcting all of the signals for the above value (see Table 1), a portion of them acquired plausible values of *BE* (in Table 1, they are boldfaced and marked with the + sign), whereas the others cannot be ascribed to any of the chemical compounds (they are marked with "?"). For the latter group of signals, plausible values of *BE* can be obtained by ascribing the second C 1*s* signal with $BE = 288.2$ eV to amorphous carbon (see Table 1). On the contrary, in this case, strange values of *BE* correspond to signals from the former group. Indeed, the initial *BE*(C 1*s*) = 292.9 eV went to 289.5 eV, which is characteristic of inorganic carbonates, after correcting for Δ_B. In particular, the value of *BE*(C 1*s*) ≈ 289 eV was reported for barium carbonate [21, 22]. If we correct the binding energy of 292.9 eV for Δ_A, the resulting value is 292.6 eV, which is close to *BE*(C 1*s*) for fluorine-containing organic molecules and unreasonably large for components that can occur as catalyst constituents. The analysis performed unambiguously demonstrates the occurrence of two phases with different conductivities. Because of the presence of these phases, the differential charging effect occurs and the photoelectron signals of the elements that constitute these phases are shifted by different values ($\Delta_A = 0.3$ eV or $\Delta_B = 3.4$ eV).

To determine the nature of phases with different conductivities in the $Pt/BaCO_3/Al_2O_3$ model catalysts, the assignment of XPS signals for other elements should be considered in more detail. There are two signals in the region of the O 1*s* spectrum (Fig. 2b). The *BE* of one of these signals corrected for Δ_B is 531.2 eV (Table 1), which is characteristic of aluminum oxides (531.1 eV). The binding energy of the other O 1*s* signal shifted by Δ_B becomes 531.1 eV, which is close to the published value of 530.8 eV for barium carbonate [21, 22].

With consideration for the correction Δ_A, *BE*(Al 2*s*) is 119.6 eV (Table 1), which corresponds to the value characteristic of Al_2O_3.

The binding energy of the more intense signal in the Ba $3d_{5/2}$ region after shifting by Δ_B becomes 779.3 eV (Table 1); that is, it is close to the value of 779.4 eV for barium carbonate [21, 22].

Thus, an analysis of the XPS spectra in the C 1*s*, O 1*s*, Al 2*s*, and Ba 3*d* regions allowed us to hypothesize that two components, Al_2O_3 and $BaCO_3$, can occur in the model catalyst. In the course of photoemission, these components acquire different potentials; as a result of this, their signals are shifted by 0.3 and 3.4 eV, respectively. Two C 1*s* signals with binding energies of 285.1 and 288.2 eV correspond to amorphous carbon, which accumulates on the surfaces of Al_2O_3 and $BaCO_3$, respectively, in the course of measuring the spectra.

Note that one more signal of lower intensity occurs in the Ba $3d_{5/2}$ region in addition to the main signal; the binding energy of this signal corrected for Δ_B is 776.5 eV, which is beyond the range of *BE*(Ba $3d_{5/2}$) for well-known Ba-containing compounds. However, this binding energy corrected for Δ_A is *BE*(Ba $3d_{5/2}$) = 779.6 eV, which corresponds to the oxidation state Ba(II). It would be hypothesized that this signal would belong to barium aluminate formed in the course of catalyst preparation. However, it is well known that $BaAl_2O_4$ is formed at temperatures of ≥850°C [23, 24], whereas we prepared the sample at 600°C. It is more reasonable to ascribe the weak Ba $3d_{5/2}$ signal to Ba^{2+} cations arranged at the interface between $BaCO_3$ and Al_2O_3. Because of the occurrence of a potential gradient at the interface, the apparent value of *BE* acquired by Ba^{2+} is lower than that in the bulk of $BaCO_3$.

Let us analyze the region of the spectrum where Pt 4*f* and Al 2*p* signals were detected (Fig. 2d). For comparison, Fig. 2d shows the spectrum of a Pt/Al_2O_3 sample, which was prepared by the thermal evaporation of platinum onto the surface of a thin alumina film not treated with a barium carbonate suspension, in addition to the spectrum of the $Pt/BaCO_3/Al_2O_3$ model catalyst. The spectrum of a Pt/Al_2O_3 exhibits a Pt $4f_{7/2}$–Pt $4f_{5/2}$ doublet, which is characterized by a signal intensity ratio of 4 : 3 and a spin–orbital splitting of 3.3 eV, and an Al 2*p* signal (dashed line in Fig. 2d). In the deconvolution of the latter, we used parameters determined with reference to another characteristic signal of aluminum, Al 2*s*. After correcting the binding energy for the position of the C 1*s* signal of amorphous carbon, *BE*(Pt $4f_{7/2}$) is 71.8 eV; that is, it falls within the range characteristic of small platinum metal particles (a few nanometers in size). The greater value of *BE*(Pt $4f_{7/2}$), as compared with that of bulk platinum (71.2 eV), can be explained by a final state effect, which accompanies photoelectron emission from small particles [25–27]. Two Pt $4f_{7/2}$–Pt $4f_{5/2}$ doublets occur in the Pt 4*f* region of the spectrum of $Pt/BaCO_3/Al_2O_3$. They can be attributed to platinum metal particles supported on Al_2O_3 (subsystem **A**) and $BaCO_3$ (subsystem **B**). With consideration for the corrections Δ_A and Δ_B, the Pt $4f_{7/2}$ binding energies in both of the subsystems are ~72 eV (Table 1); this suggests the formation of small platinum particles in either of these subsystems.

Table 2 lists the corrected values of *BE* for the main signals characteristic of the subsystems **A** (Pt/Al_2O_3) and **B** ($Pt/BaCO_3$). The assignments of all of the XPS signals in the spectrum of the initial $Pt/BaCO_3/Al_2O_3$ sample are also specified. The stoichiometric compositions of both of the subsystems were evaluated from the intensities of photoemission signals with consideration for atomic sensitivity factors [28]:

Al : O = 1 : 2.2 in Pt/Al_2O_3 (subsystem **A**);

Ba : C : O = 1 : 2.0 : 5.5 in $Pt/BaCO_3$ (subsystem **B**).

The O : Al ratio in the subsystem **A**, which is somewhat higher than the stoichiometric ratio, can be explained by the hydroxylation of the oxide surface. The atomic ratio between the elements in the subsystem **B** suggests the occurrence of barium hydrocarbonate $Ba(HCO_3)_2$ on the surface of the initial sample.

Thus, based on the analysis of the XPS spectra, we can conclude that the initial $Pt/BaCO_3/Al_2O_3$ model catalyst is a thin film of alumina, the surface of which is only partially coated with barium carbonate (Fig. 3). Platinum metal particles are located on both alumina and barium carbonate. According to XPS data, the catalyst consists of the two subsystems Pt/Al_2O_3 (**A**) and $Pt/BaCO_3$ (**B**), which differ from each other in surface charges acquired in the course of electron photoemission.

Table 2. Binding energies in the XPS spectrum of the initial $Pt/BaCO_3/Al_2O_3$ sample and the assignment of photoemission signals to corresponding chemical compounds

Signal	Pt/Al_2O_3 subsystem		$Pt/BaCO_3$ subsystem	
	binding energy, eV	assignment	binding energy, eV	assignment
C 1*s*	284.8	$C/Pt/Al_2O_3$	284.8	$C/Pt/BaCO_3$
			289.5	$CO_3^{2-}/BaCO_3$
O 1*s*	531.2	O^{2-}/Al_2O_3	531.1	$CO_3^{2-}/BaCO_3$
Al 2*s*	119.6	Al_2O_3	–	–
Ba $3d_{5/2}$	779.6	Ba^{2+}/Al_2O_3	779.3	$BaCO_3$
Pt $4f_{7/2}$	72.0	Pt/Al_2O_3	71.9	$Pt/BaCO_3$

Interaction of the $Pt/BaCO_3/Al_2O_3$ Catalyst with NO_x and the Subsequent Reducing Regeneration

Because the two subsystems (Pt/Al_2O_3 and $Pt/BaCO_3$) in the model catalyst acquire essentially different potentials in the course of electron photoemission, XPS provides an opportunity to distinguish between species of the same chemical nature located on the surfaces of different catalyst components. We used this manifestation of the differential charging effect to identify surface compounds formed by the interaction of the $Pt/BaCO_3/Al_2O_3$ model catalyst with NO_x.

Figures 4 and 5 show the XPS spectra of the initial $Pt/BaCO_3/Al_2O_3$ sample in the N 1*s*, C 1*s*, O 1*s* (Fig. 4), and Pt 4*f* (Fig. 5) regions. These spectra were measured both after the treatment of the catalyst with a mixture of NO (260 Pa) + O_2 (2600 Pa) + H_2O (525 Pa) at 250°C and after reduction with a mixture of CO (2100 Pa) + H_2O (525 Pa) at 450°C. The Pt 4*f* spectra are represented in the form obtained after subtracting the Al 2*p* signal, whose parameters were determined with reference to the parameters of the Al 2*s* signal. The scale of *BE* in Figs. 4 and 5 was calibrated using the position of the C 1*s* signal due to amorphous carbon on the surface of Pt/Al_2O_3. By this is meant that all of the signals due to subsystem **A** (Pt/Al_2O_3) in the spectra occupied their true positions and the resulting values of *BE* can be used directly to identify surface species formed in the given subsystem as a result of a particular treatment

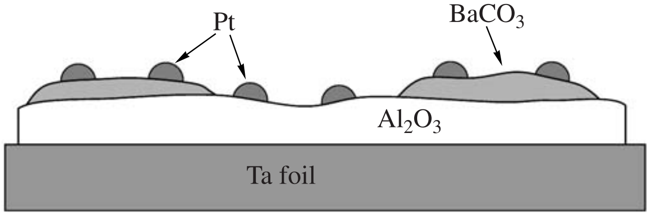

Fig. 3. $Pt/BaCO_3/Al_2O_3$ model catalyst.

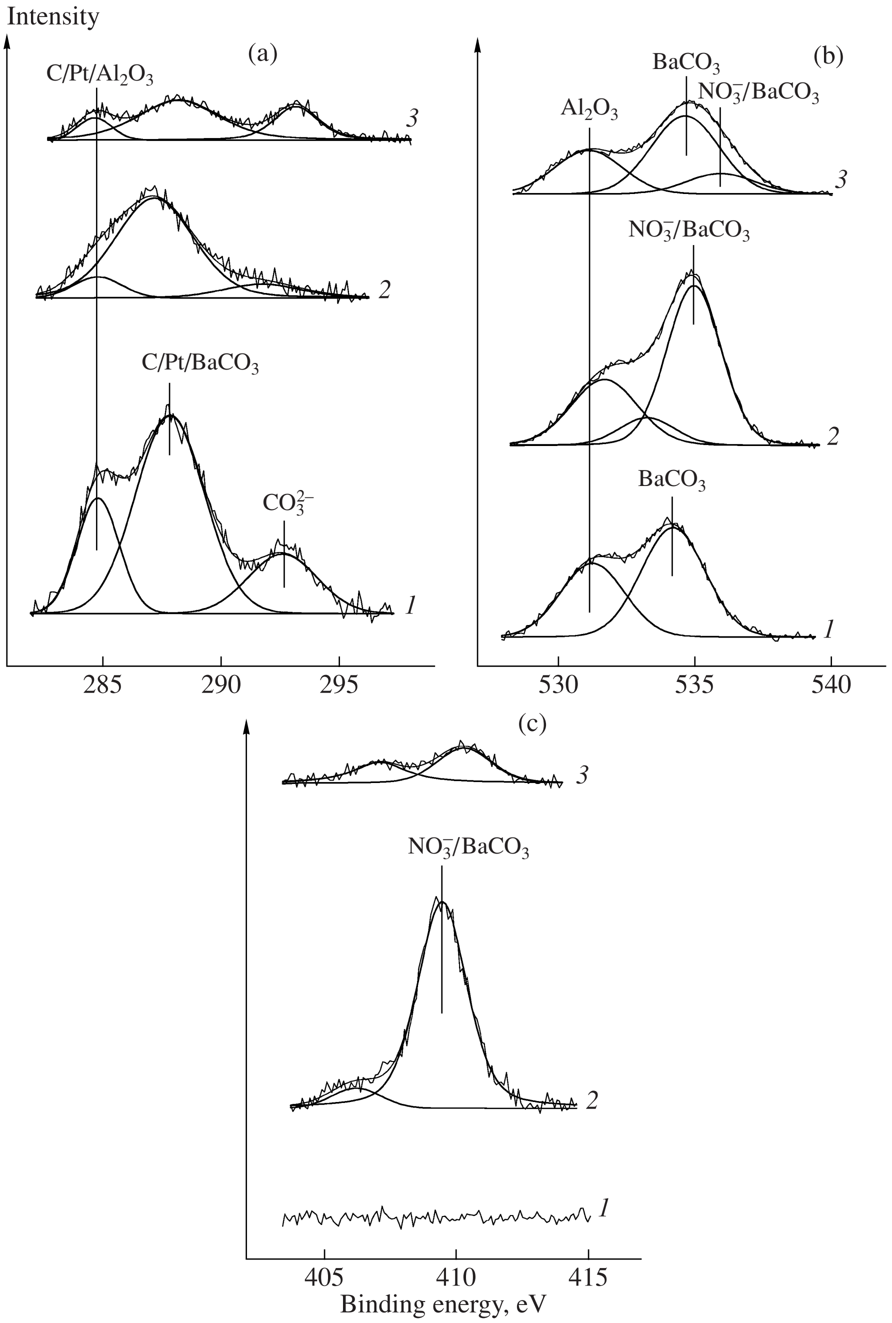

Fig. 4. (a) C 1*s*, (b) O 1*s*, and (c) N 1*s* XPS spectra of the Pt/$BaCO_3$/Al_2O_3 model catalyst (*1*) in the initial state, (*2*) after treatment with a mixture of NO (260 Pa) + O_2 (2600 Pa) + H_2O (525 Pa) at 250°C, and (*3*) after the subsequent reduction with a mixture of CO (2100 Pa) + H_2O (525 Pa) at 450°C.

(Table 3). At the same time, the signals that belong to the subsystem **B** (Pt/$BaCO_3$) were shifted by the differential charging $\Delta_B - \Delta_A$, and they should be calibrated using the C 1*s* signal of amorphous carbon that occurred in the regions of barium carbonate. Table 4 lists the values of *BE* with this correction. Tables 3 and 4 give the assignments of all of the above signals to the corresponding chemical compounds on the catalyst surface. These tables also show the directions of changes in the element concentrations of C, O, and N in the course of treatment; that is, whether they increased, decreased, or remained approximately constant.

Let us consider these changes in more detail. After the reaction with NO_x, two signals were observed in the N 1*s* region of the spectrum (Fig. 4c). The binding energy of the more intense signal, calibrated using the *BE*(C 1*s*) of amorphous carbon on the surface of Pt/$BaCO_3$, was 407.0 eV (Table 4). This allowed us to attribute it to nitrate ions on the surface of barium carbonate because *BE*(N 1*s*) in bulk $Ba(NO_3)_2$ is also 407.0 eV [21]. When we used the C 1*s* signal of the amorphous signal on the surface of Pt/Al_2O_3 as an internal standard, the binding energy of the given signal became too high to be attributed to a particular nitrogen-containing chemical compound. Thus, the attribution of the more intense N 1*s* signal is beyond question. At the same time, the nature of the product characterized by the less intense signal cannot be identified definitively. Depending on the C 1*s* signals of amorphous carbon in the Pt/Al_2O_3 and $Pt/BaCO_3$ subsystems chosen as an internal standard, this less intense signal can be ascribed to either aluminum nitrate (Table 3) or barium nitrite (Table 4), respectively. The formation of surface aluminum nitrate by the interaction of NO_x with Al_2O_3 and Pt/Al_2O_3 model systems was considered in detail elsewhere [29].

An analysis of signals recorded in other regions of the spectrum confirmed that surface barium nitrate was the main product of the interaction of $Pt/BaCO_3/Al_2O_3$ with NO_x (Fig. 4; Tables 3, 4). Two signals due to oxygen as the constituent of Al_2O_3 and $BaCO_3$ were observed in the O 1*s* spectrum of the catalyst in the initial state. These signals are separated by a considerable distance because of the differential charging effect, although the binding energies of these states of oxygen are similar (531.2 and 531.1 eV, respectively). After the interaction with NO_x, the O 1*s* signal was a superposition of three peaks, which can be attributed to aluminum oxide, barium carbonate, and barium nitrate. A small shift (0.3 eV) of the O 1*s* signal from Al_2O_3 can be explained by the formation of surface aluminum nitrate [29]. The binding energies of the other two signals, 530.8 and 535.5 eV, are consistent with the values of *BE* in bulk $BaCO_3$ and $Ba(NO_3)_2$, respectively [21]. The interaction with NO_x resulted in a decrease in the intensities of C 1*s* and O 1*s* signals due to barium carbonate (Fig. 4, Table 4). Simultaneously, *BE*(Ba $3d_{5/2}$) shifted from 779.3 to 779.7 eV (Table 4); this could also be expected in the case of the conversion of barium carbonate into the nitrate. Thus, the experimental results allowed us to conclude that nitrate ions were formed on the surface of $BaCO_3$ upon the interaction of $Pt/BaCO_3/Al_2O_3$ with NO_x at 250°C.

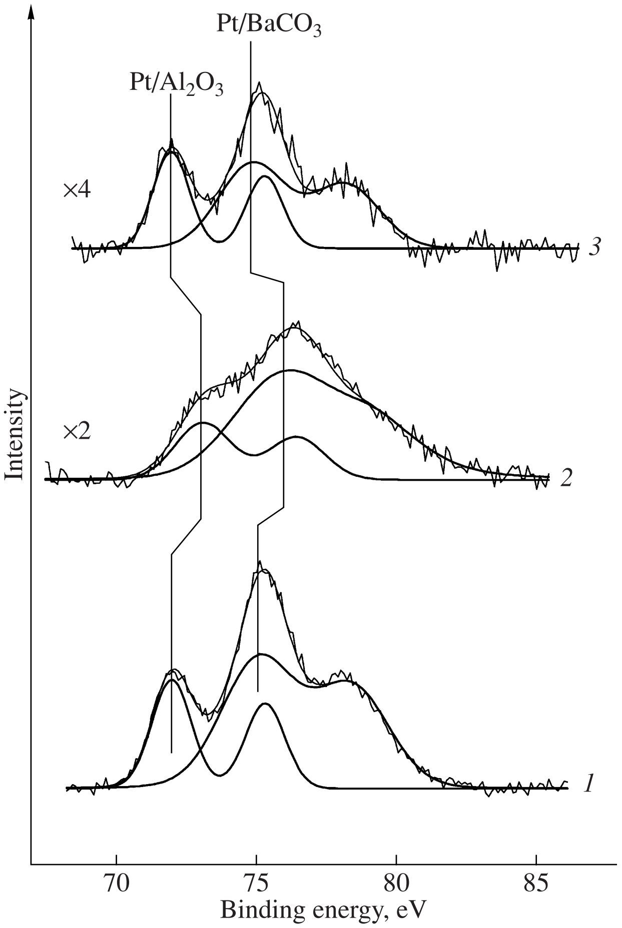

Fig. 5. Pt 4*f* XPS spectra of the $Pt/BaCO_3/Al_2O_3$ model catalyst (*1*) in the initial state, (*2*) after treatment with a mixture of NO (260 Pa) + O_2 (2600 Pa) + H_2O (525 Pa) at 250°C, and (*3*) after the subsequent reduction with a mixture of CO (2100 Pa) + H_2O (525 Pa) at 450°C.

The treatment of the model catalyst with an NO_x mixture caused not only the formation of nitrate ions on the surface of barium carbonate but also a change in the

Table 3. Binding energies in the Pt/Al_2O_3 subsystem on the surface of the $Pt/BaCO_3/Al_2O_3$ model catalyst after its treatment with an NO_x mixture at 250°C followed by reducing regeneration with a mixture of CO and H_2O at 450°C

Signal	Binding energy*, eV			Assignment
	initial sample	after interaction with NO_x	after interaction with CO + H_2O	
C 1*s*	284.8	284.8 (–)	284.8 (≈)	$C/Pt/Al_2O_3$
N 1*s*	–	406.1 (+)	407.2 (≈)	NO_3^-/Al_2O_3
O 1*s*	531.2	531.5 (≈)	531.2 (≈)	O^{2-}/Al_2O_3
Pt $4f_{7/2}$	72.0	73.1	71.9	Pt/Al_2O_3

* Directions of changes in the concentration of surface species in the course of treatment are specified in parentheses: (+), (–), and (≈) refer to increasing, decreasing, and approximately constant values, respectively.

Table 4. Binding energies in the $Pt/BaCO_3$ subsystem on the surface of the $Pt/BaCO_3/Al_2O_3$ model catalyst after its treatment with an NO_x mixture at 250°C followed by reducing regeneration with a mixture of CO and H_2O at 450°C

Signal	Binding energy*, eV			Assignment
	initial sample	after interaction with NO_x	after interaction with CO + H_2O	
C 1*s*	284.8	284.8 (–)	284.8 (≈)	$C/Pt/BaCO_3$
	289.5	289.3 (–)	289.7 (+)	$CO_3^{2-}/BaCO_3$
N 1*s*	–	403.8 (+)	403.7 (≈)	$NO_2^-/BaCO_3$
	–	407.0 (+)	406.9 (–)	$NO_3^-/BaCO_3$
O 1*s*	531.1	530.8 (–)	531.2 (+)	$CO_3^{2-}/BaCO_3$
	–	532.5 (+)	532.5 (–)	$NO_3^-/BaCO_3$
Ba $3d_{5/2}$	779.3	779.7	779.3	$BaCO_3$
Pt $4f_{7/2}$	71.9	73.5	71.5	$Pt/BaCO_3$

* Directions of the changes in the concentration of surface species in the course of treatment are specified in parentheses: (+), (–), and (≈) refer to increasing, decreasing, and approximately constant values, respectively.

chemical state of supported platinum particles (Fig. 5). Two Pt $4f_{7/2}$–Pt $4f_{5/2}$ doublets can be recognized in the Pt 4*f* spectra; they are indicative of the presence of platinum on the surfaces of Al_2O_3 and $BaCO_3$. Because the positions of the spectra are specified with reference to the C 1*s* signal of amorphous carbon on the surface of Pt/Al_2O_3, the position of the signal due to platinum on barium carbonate does not correspond to the true value of *BE* for this portion of supported platinum, which is given in Table 4. It can be seen that, upon the interaction with NO_x, the Pt 4*f* signals broadened and shifted toward greater binding energies and their intensities decreased. After treatment with an NO_x mixture, *BE*(Pt $4f_{7/2}$) was 73.1 or 73.5 eV for Pt/Al_2O_3 or $Pt/BaCO_3$, respectively (Tables 3, 4); this suggests the oxidation of platinum particles on both of the supports. The above values of *BE*(Pt $4f_{7/2}$) occupy an intermediate position between the values characteristic of the bulk oxides PtO (72.4–72.8 eV) and PtO_2 (74.2–74.6 eV) [30, 31]. It is likely that the decrease in the Pt 4*f* signal intensities with temperature was due to the agglomeration of platinum particles, although the encapsulation of these particles by products of the reaction of NO_x with the support also could take place.

After the reducing regeneration of the $Pt/BaCO_3/Al_2O_3$ sample treated with an NO_x mixture, the N 1*s* signal intensity of barium nitrate dramatically decreased, whereas the C 1*s* signal intensity of barium carbonate increased (Fig. 4). Simultaneously, the signal intensity of surface barium nitrate in the O 1*s* spectrum also decreased and the signal intensity of barium carbonate increased, whereas the Ba $3d_{5/2}$ signal shifted from 779.7 to 779.3 eV (Table 4). These changes suggest that barium nitrate was converted into the carbonate upon the treatment of the model catalyst with a mixture of CO + H_2O at 450°C.

After reducing regeneration, the Pt $4f_{7/2}$ signals shifted toward lower binding energies (Fig. 5). In the Pt/Al_2O_3 and $Pt/BaCO_3$ subsystems, *BE*(Pt $4f_{7/2}$) became 71.9 and 71.5 eV, respectively (Tables 3, 4). This suggests the reduction of platinum oxides formed at the stage of the catalyst interaction with NO_x. A further decrease in the intensities of both Pt 4*f* signals suggests the agglomeration of Pt particles; this effect was more significant for platinum supported on $BaCO_3$. The stronger agglomeration of Pt particles on the surface of $BaCO_3$ is consistent with a lower value of *BE*(Pt $4f_{7/2}$).

Thus, by XPS studies performed on the $Pt/BaCO_3/Al_2O_3$ NSR catalyst, we found the differential charging effect, which allowed us to independently examine two subsystems in the catalyst: $Pt/BaCO_3$ and Pt/Al_2O_3. The surface charge accumulated in either of the subsystems as a result of photoelectron emission can be evaluated by calibration using the position of the C 1*s* signal due to amorphous carbon on the surfaces of Pt/Al_2O_3 and $Pt/BaCO_3$. The use of the differential charging effect enabled us to identify surface compounds formed in the interaction of the model catalyst with an NO_x mixture and in the subsequent reducing regeneration with a mixture of CO with H_2O and to demonstrate that the interaction with NO_x at 250°C resulted in the conversion of carbonate ions on the surface of $BaCO_3$ into nitrate ions. In addition, the oxidation of platinum particles occurred on the surfaces of both Al_2O_3 and $BaCO_3$. The subsequent catalyst reduction at 450°C was accompanied by the decomposition of surface barium nitrate, the regeneration of a carbonate coating, and the reduction of oxidized platinum particles to a metallic state.

REFERENCES

1. Matsumoto, S., *CATTECH*, 2000, vol. 4, p. 102.
2. Epling, W.S., Campbell, L.E., Yezerets, A., Currier, N.W., and Parks, J.E., *Catal. Rev.*, 2004, vol. 46, p. 163.
3. Westerberg, B. and Fridell, E., *J. Mol. Catal. A: Chem.*, 2001, vol. 165, p. 249.
4. Szanyi, J., Kwak, J.H., Kim, D.H., Burton, S.D., and Peden, C.H.F., *J. Phys. Chem. B*, 2005, vol. 109, p. 27.
5. Nova, I., Castoldi, L., Lietti, L., Tronconi, E., Forzatti, P., Prinetto, F., and Ghiotti, G., *J. Catal.*, 2004, vol. 222, p. 377.
6. Sedlmair, C., Seshan, K., Jentys, A., and Lercher, J.A., *J. Catal.*, 2003, vol. 214, p. 308.
7. Schmitz, P.J. and Baird, R.J., *J. Phys. Chem. B*, 2002, vol. 106, p. 4172.
8. Nova, I., Castoldi, L., Prinetto, F., Dal, SantoV., Lietti, L., Tronconi, E., Forzatti, P., Ghiotti, G., Psaro, R., and Recchia, S., *Top. Catal.*, 2004, vols. 30–31, p. 181.
9. Fridell, E., Persson, H., Westerberg, B., Olsson, L., and Skoglundh, M., *Catal. Lett.*, 2000, vol. 66, p. 71.
10. *Practical Surface Analysis by Auger and X-ray Photoelectron Spectroscopy*, Briggs, D. and Seah, M.P., Eds., Chichester: Wiley, 1983.
11. Lietti, L., Forzatti, P., Nova, I., and Tronconi, E., *J. Catal.*, 2001, vol. 204, p. 175.
12. Rodrigues, F., Juste, L., Potvin, C., Tempere, J.F., Blanchard, G., and Djega-Mariadassou, G., *Catal. Lett.*, 2001, vol. 72, p. 59.
13. Eberhardt, M., Riedel, R., Gobel, U., Theis, J., and Lox, E.S., *Top. Catal.*, 2004, vols. 30–31, p. 135.
14. Bukhtiyarov, V.I., Prosvirin, I.P., and Kvon, R.I., *J. Electron Spectrosc. Relat. Phenom.*, 1996, vol. 77, p. 7.
15. Bukhtiyarov, V.I., Prosvirin, I.P., Kvon, R.I., Goncharova, S.N., and Bal'zhinimaev, B.S., *J. Chem. Soc., Faraday Trans.*, 1997, vol. 93, p. 2323.
16. Jaramillo, A., Spurlock, L.D., Young, V., and Brajter-Toth, A., *Analyst*, 1999, vol. 124, p. 1215.
17. Shabtai, K., Rubinstein, I., Cohen, S.R., and Cohen, H., *J. Am. Chem. Soc.*, 2000, vol. 122, p. 4959.
18. Suzer, S., *Anal. Chem.*, 2003, vol. 75, p. 7026.
19. Ulgut, B. and Suzer, S., *J. Phys. Chem. B*, 2003, vol. 107, p. 2939.
20. Dubey, M., Gouzman, I., Bernasek, S.L., and Schwartz, J., *Langmuir*, 2006, vol. 22, p. 4649.
21. Christie, A.B., Lee, J., Sutherland, I., and Walls, J.M., *Appl. Surf. Sci.*, 1983, vol. 15, p. 224.
22. Miot, C., Husson, E., Proust, C., Erre, R., and Coutures, J.P., *J. Mater. Res.*, 1997, vol. 12, p. 2388.
23. Jang, B.H., Yeon, T.H., Han, H.S., Park, Y.K., and Yie, J.E., *Catal. Lett.*, 2001, vol. 77, p. 21.
24. Capasu, M., Grunwaldt, J.-D., Maciejewski, M., Wittrock, M., Gobel, U., and Baiker, A., *Appl. Catal., B*, 2006, vol. 63, p. 232.
25. Huizinga, T., Blik, H.F.J., Vis, J.C., and Prins, R., *Surf. Sci.*, 1983, vol. 135, p. 580.
26. Parmigiani, F., Kay, E., Bagus, P.S., and Nelin, C.J., *J. Electron Spectrosc. Relat. Phenom.*, 1985, vol. 36, p. 257.
27. Steinruck, H.-P., Pesty, F., Zhang, L., and Madey, T.E., *Phys. Rev. B: Condens. Matter*, 1995, vol. 51, p. 2427.
28. Moulder, J.F., Stickle, W.F., Sobol, P.E., and Bomben, K.D., *Handbook of X-ray Photoelectron Spectroscopy*, PerkinElmer, 1992.
29. Smirnov, M.Yu., Kalinkin, A.V., and Bukhtiyarov, V.I., *Zh. Strukt. Khim.*, 2007, vol. 48, p. 1120 [*J. Struct. Chem.* (Engl. Transl.), vol. 48, p. 1053].
30. Kaushik, V.K., *Z. Phys. Chem.*, 1991, vol. 173, p. 105.
31. Zafeiratos, S., Papakonstantinou, G., Jacksic, M.M., and Neophytides, S.G., *J. Catal.*, 2005, vol. 232, p. 127.